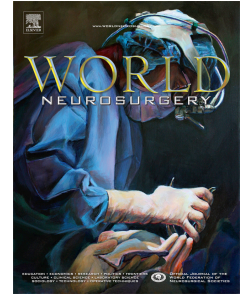


Journal Pre-proof



A Novel Approach to Percutaneous Lumbar Surgeries via Kambin's Triangle - A Radiographic and Surgical Planning Analysis with Nerve Segmentation Technology

Troy Q. Tabarestani, BA, David A.W. Sykes, AB, Romaric W. Kouam, RN, MSc, David S. Salven, BS, MS, Timothy Y. Wang, MD, Vikram A. Mehta, MD, MPH, Christopher I. Shaffrey, MD, Walter F. Wiggins, MD, PhD, John H. Chi, MD, MPH, Muhammad M. Abd-El-Barr, MD, PhD

PII: S1878-8750(23)00830-6

DOI: <https://doi.org/10.1016/j.wneu.2023.06.061>

Reference: WNEU 20724

To appear in: *World Neurosurgery*

Received Date: 12 June 2023

Accepted Date: 15 June 2023

Please cite this article as: Tabarestani TQ, Sykes DAW, Kouam RW, Salven DS, Wang TY, Mehta VA, Shaffrey CI, Wiggins WF, Chi JH, Abd-El-Barr MM, A Novel Approach to Percutaneous Lumbar Surgeries via Kambin's Triangle - A Radiographic and Surgical Planning Analysis with Nerve Segmentation Technology, *World Neurosurgery* (2023), doi: <https://doi.org/10.1016/j.wneu.2023.06.061>.

This is a PDF file of an article that has undergone enhancements after acceptance, such as the addition of a cover page and metadata, and formatting for readability, but it is not yet the definitive version of record. This version will undergo additional copyediting, typesetting and review before it is published in its final form, but we are providing this version to give early visibility of the article. Please note that, during the production process, errors may be discovered which could affect the content, and all legal disclaimers that apply to the journal pertain.

© 2023 Elsevier Inc. All rights reserved.

A Novel Approach to Percutaneous Lumbar Surgeries via Kambin's Triangle - A Radiographic and Surgical Planning Analysis with Nerve Segmentation Technology

Authors: Troy Q. Tabarestani, BA¹, David A.W. Sykes, AB¹, Romaric W. Kouam, RN, MSc², David S. Salven, BS, MS¹, Timothy Y. Wang, MD³, Vikram A. Mehta, MD, MPH³, Christopher I. Shaffrey, MD³, Walter F. Wiggins, MD, PhD⁴, John H. Chi, MD, MPH⁵, Muhammad M. Abd-El-Barr, MD, PhD³

¹Duke University School of Medicine, Durham, NC, USA

²Campbell University School of Osteopathic Medicine, Lillington, NC, United States

³Department of Neurosurgery, Duke University Hospital, Durham, NC, USA

⁴Department of Radiology, Duke University Hospital, Durham, NC, USA

⁵Department of Neurosurgery, Brigham and Women's Hospital, Boston, MA, USA

Corresponding Author:

Troy Q. Tabarestani, BA

Duke University School of Medicine

2610 Erwin Road

Durham, NC 27705

Email: tqt5@duke.edu

Twitter: @QTabarestani

Keywords: Exiting nerve root, Kambin's triangle, lumbar interbody fusion, MRI/CT fusion, percutaneous, 3D imaging segmentation, spondylolisthesis, disc space height, minimally invasive, dorsal root ganglion

Previous Presentations: This work was presented via Zoom at the 1st NeuroSpine Zoom Research forum on February 3rd, 2023.

Funding and Disclosures: No funding was received for this research. Dr. Abd-El-Barr is a consultant for Spineology, TrackX, and Depuy. There are no other relevant disclosures pertaining to the content of this manuscript.

Short Title: Nerve Segmentation for perCLIF Planning

1 **Abstract:**

2 **Objective:** While Kambin's triangle has become an ever more important anatomic window given
3 its proximity to the exiting nerve root, there have been limited studies examining the effect of
4 disease on the corridor. Our goal was to better understand how pathology can affect Kambin's
5 triangle thereby altering laterality of approach for percutaneous lumbar interbody fusion
6 (perCLIF).

7 **Methods:** The authors performed a single-center retrospective review of patients evaluated for
8 perCLIF. The areas of Kambin's triangle were measured without and with nerve segmentation.
9 For the latter, the lumbosacral nerve roots on 3D T2 MRI were manually segmented. Next, the
10 borders of Kambin's triangle were delineated ensuring no overlap between the area and the nerve
11 above.

12 **Results:** 15 patients (67.5 ± 9.7 years, 46.7% female) were retrospectively reviewed. 150
13 Kambin's triangles were measured. The mean areas from L1-S1 were 50.0 ± 12.3 mm², $73.8 \pm$
14 12.5 mm², 83.8 ± 12.2 mm², 88.5 ± 19.0 mm², and 116 ± 29.3 mm², respectively. When
15 pathology was present, the areas significantly decreased at L4-L5 ($p = 0.046$) and L5-S1 ($p =$
16 0.049). Higher spondylolisthesis and smaller posterior disc heights were linked with decreased
17 areas via linear regression analysis ($p < 0.05$). When nerve segmentation was used, the areas
18 were significantly smaller from L1-L5 ($p < 0.05$). Among 11 patients who underwent surgery,
19 none suffered from postoperative neuropathies.

20 **Conclusion:** These results illustrate the feasibility of pre-operatively segmenting lumbosacral
21 nerves and measuring Kambin's triangle to help guide surgical planning and determine the ideal
22 laterality of approach for perCLIF.

23

24 **Introduction:**

25 A procedure that has continued to gain traction for the treatment of degenerative
26 spondylolisthesis or disc disease is the percutaneous lumbar interbody fusion (perCLIF) through
27 Kambin's triangle.^{1,2} Kambin's triangle is an anatomical corridor that provides safe access to the
28 disc space.³⁻⁵ Currently, the triangle is defined as the exiting nerve root (ENR), superior endplate
29 of the caudal vertebral body, and superior articulating process. However, there is still significant
30 variation regarding the dimensions, angles of entry, and borders of Kambin's triangle.^{6,7}

31 The importance of quantifying the size of Kambin's triangle is crucial since minimally
32 invasive surgeries (MIS) have been linked with higher rates of nerve root injuries compared with
33 conventional open surgery.⁸ ENR injuries are the most common complication of the perCLIF
34 with rates as high as 20% having been reported in the literature.⁸ A recent systematic review
35 highlighted that at a pathologic level, there may be a significant decrease in the area of Kambin's
36 triangle compared to healthy levels.⁹ Thus, there is an ever-present risk for injury to the ENR,
37 theca, and the dorsal root ganglion (DRG) during disc entry and endplate preparation.

38 Previous methods for the perCLIF have relied heavily on fluoroscopy, computed
39 tomography (CT) imaging, and triggered nerve stimulation. However, there remains no well-
40 established strategies to plan a three-dimensional (3D) trajectory into the disc with knowledge of
41 where the important neural structures are. Although still in its early technological stages,
42 segmentation software was used in this small cohort study in an attempt to address these
43 shortcomings with a novel technique of merging preoperatively segmented magnetic resonance
44 imaging (MRI) with an intraoperative CT. This study's goals were 1) to better understand the
45 dimensional trends in Kambin's triangle, 2) understand how segmentation of the ENR affects the
46 area, 3) identify how pathologies can affect its area, and 4) illustrate the importance of

47 preoperatively visualizing the triangle in 3D to determine the ideal laterality of disc space
48 entrance.

49

50 **Materials and Methods**

51 *Study Design*

52 The authors performed a single-center retrospective review of patients being evaluated
53 for perCLIF at a major academic research institution. From August 2021 - March 2023, patients
54 were included according to the established indications for perCLIF in the literature. Informed
55 consent was obtained before every procedure. Patient permission to publish deidentified data was
56 not necessary, as this study fell under the university's IRB's guidelines for "exempt" patient
57 research. Data was collected via electronic health record review. Spondylolisthesis, anterior disc
58 height (ADH), and posterior disc height (PDH) were measured using pre-operative radiographs.

59

60 *Kambin's Triangle without ENR Segmentation*

61 3D isotropic T2-weighted MRI sequences acquired at 1-mm slice thickness were used
62 during the preoperative planning phase (Figure 1). The *Align* feature in BrainLab (BrainLab,
63 Munich, Germany) was used to orient the images (coronal, axial, and sagittal) in the direction
64 that maximized the cross-sectional area of Kambin's triangle. The triangle was then outlined
65 using *Smartbrush* without the aid of the ENR (Figure 2). A board-certified neuroradiologist
66 confirmed each segmentation. We used an approximation of the largest triangle that contained
67 every part of the outlined space and calculated the area using the formula: $0.5 \times \text{base} \times \text{height}$.

68

69 *Kambin's Triangle with ENR Segmentation*

70 In contrast to the prior method, individual ENRs were identified first in the axial and then
71 sagittal plane with *Smartbrush* completing segmentation based on a region-growing algorithm
72 (Figure 3). Each ENR was ‘drawn out’ bilaterally starting from where it exited the spinal cord to
73 as far lateral as possible. Once the nerves were visualized, the *Align* feature was again used to
74 orient the images to maximize the cross-sectional area of Kambin’s triangle (Figure 4). Since the
75 ENR had already been segmented, it helped ensure that we were not overlapping Kambin’s
76 triangle with any part of the nerve. To measure area, we used the same triangle approximation
77 and formula stated above (Figure 5). BrainLab then generated a 3D representation of the
78 structures to visualize spatial proximity (Figure 6).

79

80 *Operative Management*

81 We have recently reported the perioperative outcomes of our first 5 patients.¹⁰ Every
82 patient had free running electromyography (EMG), which was monitored via electrodes placed
83 in selected muscles of the bilateral lower extremities. Pedicle screws were placed at the proper
84 levels using instrument-tracking previously described by our group (Figure 7).^{11,12} A
85 percutaneous patient reference array was then placed in the patient’s posterior superior iliac crest
86 (PSIS) using two 4 mm Schanz screws. An intraoperative CT (AIRO, Kalamazoo, Michigan)
87 was then merged with the preoperative segmented MRI, with the help of a vendor representative
88 from BrainLab. The CT scan, depending on the operative level, was done to include all five
89 lumbar levels as well as portions of the sacrum to increase the accuracy of the fusion. A region
90 of interest (ROI) was selected at the operative level, and the elastic fusion was centered around
91 the accuracy of overlap in the ROI (Figure 8). This process focused the fusion on the most
92 surgically-relevant level, given that the remaining vertebrae may have shifted due to the altering

93 in patient positioning from the supine preoperative MRI to the prone intraoperative CT. Having
94 said this, all levels were lined up as accurately as possible during the elastic fusion process. Safe
95 trajectories entering the disc space at the mid-pedicle point on coronal imaging were then
96 planned (Figure 9). Based on the preoperative measurements of Kambin's triangle and the
97 planned trajectory, an incision approximately 6 cm lateral of the midline was made based on
98 which side had the larger triangle. A stimulating dilator (Spineology, St. Paul, MN) was then
99 used to pierce into the annulus of the desired disc using the preplanned trajectory and BrainLab
100 navigation (Figure 7). As long as no compound muscle action potentials in the lower extremities
101 were recorded during activation of a threshold of 4 mA, it was felt that a 'safe' trajectory was
102 used.^{13,14} After appropriate discectomy, the ELITE expandable titanium cage (Spineology, St.
103 Paul, MN) was placed and expanded. Bilateral rods connected the screws for fusion (Figure 7).

104

105 *Statistical Analysis*

106 For all continuous variables, a two sample t-test was conducted where $p < 0.05$ was
107 considered statistically significant. For linear regressions, analysis was done with the built-in
108 Excel[®] (Redmond, Washington) data analysis tool pack using an ANOVA model.

109

110 **Results**

111 *Trends in Kambin's triangle with and without nerve segmentation*

112 Fifteen patients (67.5 ± 9.7 years, 46.7% female, BMI 29.3 ± 5.22 kg/m²) were included.
113 In total, 150 Kambin's triangles were individually segmented and measured using the triangle
114 approximation method. The mean areas at L1-L2, L2-L3, L3-L4, and L5-S1 were 50.0 ± 12.3
115 mm², 73.8 ± 12.5 mm², 83.8 ± 12.2 mm², 88.5 ± 19.0 mm², and 116 ± 29.3 mm², respectively

116 (Table 1). The data was uniformly distributed at each level. The dimensional trend of the area
117 followed a linear regression model ($p = 0.007$, $R^2 = 0.94$) revealing a significant increase in size
118 going down the lumbar spine. Upon comparing the two different approaches, the calculated areas
119 of Kambin's triangle were significantly smaller from L1-L5 ($p < 0.05$), but not at L5-S1 ($p =$
120 0.29) when the triangle was outlined with the aid of the ENR segmentation (Figure 10).

121

122 *Pathology can significantly reduce Kambin's triangle*

123 The most common pathology was Grade 1 spondylolisthesis (80%), followed by
124 foraminal stenosis (46.7%), and then Grade 2 spondylolisthesis (13.3%) (Table 2). When any of
125 these pathologies were present, the area of Kambin's triangle significantly decreased at L4-L5 (p
126 $= 0.046$) and L5-S1 ($p = 0.049$). (Table 3). At these pathologic operative levels, there was also a
127 significant difference in sizes between the smaller and larger Kambin's triangle at the L4-L5
128 level. Among the 12 patients who had pathology at the L4-L5 level, the mean area for the
129 smaller Kambin's triangle was $76.2 \pm 14.5 \text{ mm}^2$ while the mean of the larger Kambin's triangle
130 was $93.9 \pm 15.9 \text{ mm}^2$, which was significantly larger ($p = 0.0091$) (Table 4). One patient had a
131 conjoined nerve root of the right L5-S1 nerve (Figure 11). When comparing the right and left
132 triangles at that level, the presence of the conjoined nerve root drastically reduced the area of
133 Kambin's triangle by 46.4 mm^2 (38.3%).

134 Next, when plotting the radiographic variables against the area of Kambin's triangle,
135 linear regression analysis revealed two key findings: 1) Higher values for spondylolisthesis were
136 significantly associated with smaller areas of Kambin's triangle across all lumbar levels ($R^2 =$
137 0.095 , $p = 0.0083$); 2) lower measurements of PDH were also associated with smaller areas of
138 the triangle ($R^2 = 0.063$, $p = 0.033$). ADH did not show any association with the area.

139

140 *Peri- and Postoperative data*

141 In terms of perioperative data, 11 (73.3%) patients from the total cohort have undergone
142 their planned surgery at this point in time.¹⁰ Among them, the most commonly operated on level
143 was L4-L5 (81.8%). Only two patients underwent a multilevel fusion from L4-S1. 6 (54.5%)
144 patients underwent 'awake' surgery while the remaining had general anesthesia. The mean
145 estimated blood loss was 57.7 ± 47.8 mL, the median operative time was 174 minutes with a
146 range of 140 – 210 minutes, and the mean length of stay in the hospital was 28.2 ± 11.2 hours.
147 There were no intraoperative or postoperative complications noted for any of the cohort. None of
148 the patients suffered from motor or sensory deficits at a mean postoperative follow-up of $8.90 \pm$
149 4.94 months (Table 5).

150

151 **Discussion**

152 An ENR can be injured in two main ways: (1) during blind manipulation while inserting
153 a k-wire, obturator, or cannula, or (2) from excessive pressure exerted by the
154 instruments. Morgenstern and Morgenstern reported a 32% postoperative complication rate
155 consisting of ipsilateral dysesthesias and transitory muscle weakness following trans-Kambin
156 procedures.¹⁵ Similarly, studies have shown that postoperative dysesthesia should be expected in
157 one-fifth of patients following transforaminal endoscopic decompression, which was attributed
158 to DRG irritation.¹⁶ More recent work has shown a decrease in the overall complication rate
159 following percutaneous surgeries, but Choi et al. reported that the rate of ENR injury increased
160 by 23% for each 1-mm decrease in distance from the nerve root to the facet joint of the lower
161 level.^{17,18} Of note, these previous studies that report ENR injury either did not measure the area

162 of Kambin's triangle preoperatively or measured it retrospectively after the operation. In order to
163 reduce the prevalence of these injuries, our approach uses manual nerve root segmentation to
164 both preoperatively measure Kambin's triangle and plan a safe path into the disc space.

165 *MRI/CT fusion is the future of surgical planning*

166 Over the last several years, researchers have begun testing the limits of MRI and CT 3D
167 segmentation technology in both a manual and automated setting, the latter facilitated by
168 advances in machine learning.¹⁹ Although there has not been a comparable study in the literature
169 that has measured all the lumbar levels using CT, Fan et al. used a CT deep-learning model
170 specifically for the L5-S1 level.²⁰ Their mean area was ~150 mm², which was much larger than
171 our mean area of 116 mm² for the same level. This lack of adequate ENR visualization on CT
172 may result in an overestimation of the triangle's area thereby giving surgeons a false sense of
173 security when entering the disc space. We attempted to test this hypothesis by performing our
174 analysis of the triangle's area with and without ENR segmentation. As expected, when trying to
175 locate the largest area for Kambin's triangle without the aid of the segmented nerve root acting
176 as the hypotenuse, it is much more difficult to accurately pinpoint the appropriate borders when
177 outlining the corridor. Especially when viewed in only two dimensions, it is challenging to
178 ensure that the estimated area of the triangle does not overlap by more distal portions of the ENR
179 as it traverses away from the spine. Although the surgical implications of this difference have not
180 been studied, it is reasonable to speculate that using either CT or MRI scans without prior ENR
181 segmentation may lead to an overestimation of the safe zone. This may thereby affect the
182 dimensions of cannulas that can be safely used intraoperatively. Given the small cohort in this

183 work, these preliminary conclusions will need further testing using large scale prospective
184 studies.

185 As a result, research have begun shifting more towards MRI segmentation.²¹ Pairaiturkar
186 et al. used 3D MRI of Kambin's safe zone to find the maximum cannula diameter permissible for
187 safe percutaneous endoscopic lumbar discectomy.¹⁷ Although they did not directly calculate the
188 areas of each triangle, their results paralleled ours. Mainly, they showed that the distance from
189 the ENR to the facet joint increased going down the lumbar spine, further corroborating our data.
190 Consequently, they concluded that the maximum diameter of an endoscopic cannula permissible
191 through Kambin's triangle was highest at L5-S1 (6.11 mm) with the smallest diameter being at
192 L1-L2 (4.03 mm). While they also measured both the right and left triangles, they did not
193 mention any significant differences between the sides of entry or mention how pathology could
194 affect the diameters.¹⁷

195

196 *Presence of pathology can decrease Kambin's Triangle*

197 Many of these prior works examining the efficacy of 3D segmentation concentrated on
198 intact anatomy of Kambin's triangle, but there has yet to be a dedicated study examining the
199 effect of disease on the dimensions of the triangle. We found that Kambin's triangle at a
200 pathological level was significantly smaller than non-pathological levels, indicating that the
201 presence of disease or degeneration could play a key factor in the variability of the area and
202 should be taken into account during pre-operative planning. Specifically, there was a 23.3 mm²
203 difference in average area between the diseased and healthy levels of L5-S1. This may be the
204 explanation as to why some researchers have discouraged the percutaneous entrance into L5-S1
205 without foraminoplasty.^{22,23} Our findings align appropriately with prior research done by Waguia

206 Kouam et al., who revealed similar trends in both the overall area and potential changes at the
207 operative levels in their meta-analysis.⁵ We took the analysis one step further by comparing the
208 left and right Kambin's triangle at these diseased levels to determine if there was a significant
209 difference between sides. At the L4-L5 level, which was the most commonly diseased, there was
210 a 17.8 mm² (20.9%) difference between sides. This significant increase in area allowed the
211 surgical team to preoperatively pick the laterality of approach that maximized the working zone
212 they had to enter the disc space, thereby reducing the chance of ENR and DRG irritation.
213 Hirayama et al. performed a similar analysis to determine the optimal angle of entry, but they did
214 not speak on identifying the laterality of approach for an individual patient.²⁴

215 Given that there is no current literature researching the possible association between
216 radiographic variables and Kambin's triangle, we recorded spondylolisthesis, ADH, and PDH,
217 which are all common factors measured during the pre-operative workup for patients. Our results
218 illustrated a potential link between higher values for spondylolisthesis and lower values for PDH
219 with smaller areas of Kambin's triangle. Anatomically, this association makes sense since the
220 disc height is inherently built in as part of the medial border of Kambin's triangle. However, the
221 effect of spondylolisthesis requires further investigation with larger cohorts, especially given that
222 it was the most common pathology present among lumbar surgeries in general.^{25,26}

223 Not only is there variability when pathology is present, but congenital malformations of
224 the surrounding bony and neurovascular structures may increase the need for more accurate
225 preoperative segmentation.²⁷ As illustrated in Figure 11, the presence of the conjoined nerve root
226 significantly reduced the safe zone of Kambin's triangle by almost 50 mm². Haijiao et al. found a
227 17% incidence of nerve root anomalies out of 376 lumbar MRI scans, whereas prior studies
228 relied mainly on CT scans, which only caught 2% of the conjoined roots.^{28,29} Accordingly, there

229 would have been a risk of overlooking this anomaly if only CT imaging was used, thereby
230 increasing the risk for ENR damage.

231

232 *Limitations*

233 This study had several limitations. First and foremost, the sample size was small, so
234 making general conclusions about our work would require studies with larger cohorts. Likewise,
235 the retrospective nature of the study brings inherent bias for both the data analysis and
236 generalizability of our findings. The main reason for the small number of patients is the relative
237 novelty of using this technique at our institution. To counterbalance this, all the lumbar levels for
238 each patient were segmented bilaterally, which increased the number of total analyzed levels to
239 150 for heightened statistical power. This study aims to show the feasibility of implementing this
240 nerve segmentation technology effectively in the operating room. Given that there have been no
241 prior studies examining this topic, we believe that this work can be a stepping stone for future
242 prospective studies looking at the correlation between segmentation, pathology, and the safe area
243 of the triangle.

244 Second, although a board-certified neuroradiologist confirmed each of the segmentations,
245 there is still inherent bias when segmenting the areas. It is also possible that patient positioning
246 may impact the location of the ENR. It would be interesting to analyze the effects of patient
247 positioning on Kambin's triangle, but this would require an intraoperative MRI prior to
248 instrumentation placement. Third, we are limited by the length of follow-up for these patients,
249 given that this technique was only recently adopted at our institution. In terms of operative time,
250 these procedures did fall on the higher end of average when compared to their open and MIS
251 single-level fusion counterparts, which have been estimated to last between 120 – 180 minutes.³⁰

252 We hypothesize that with further experience and more cases performed, operative times will
253 decrease as surgeons climb the learning curve.

254

255 **Conclusion**

256 In this small retrospective cohort study, we created 3D images by manually segmenting
257 lumbar ENR from preoperative MRI using commercially available software and merging them
258 with intraoperative CT images. The 3D images allowed us to preoperatively measure the area of
259 Kambin's triangle without overlapping with the ENR, determine the ideal laterality of approach
260 to maximize the safe zone, and plan a trajectory for percutaneous spinal surgery. We found that
261 although there is a linear increase in the area going down the lumbar spine, the presence of
262 pathology and using the preemptive nerve segmentation technique can significantly reduce the
263 area of Kambin's triangle. Further prospective studies will be needed to corroborate our
264 preliminary findings on a larger, more widespread scale.

265

266 **Acknowledgements:** We would like to acknowledge the Duke University Statistics department
267 for helping with our analysis.

268

269 **References**

- 270 1. Wang TY, Mehta VA, Gabr M, et al. Percutaneous Lumbar Interbody Fusion With an
271 Expandable Titanium Cage Through Kambin's Triangle: A Case Series With Initial Clinical and
272 Radiographic Results. *Int J Spine Surg*. Dec 2021;15(6):1121-1129. doi:10.14444/8144

- 273 2. Wang MY, Grossman J. Endoscopic minimally invasive transforaminal interbody fusion
274 without general anesthesia: initial clinical experience with 1-year follow-up. *Neurosurg Focus*.
275 Feb 2016;40(2):E13. doi:10.3171/2015.11.Focus15435
- 276 3. Fanous AA, Tumialán LM, Wang MY. Kambin's triangle: definition and new
277 classification schema. *Journal of Neurosurgery: Spine SPI*. 01 Mar. 2020 2020;32(3):390-398.
278 doi:10.3171/2019.8.Spine181475
- 279 4. Kumari C, Gupta T, Gupta R, et al. Cadaveric anatomy of the lumbar triangular safe zone
280 of Kambin's in North West Indian population. *Anat Cell Biol*. Mar 31 2021;54(1):35-41.
281 doi:10.5115/acb.20.243
- 282 5. Waguia Kouam R, Tabarestani TQ, Sykes DAW, et al. How dimensions can guide
283 surgical planning and training: a systematic review of Kambin's triangle. *Neurosurg Focus*. Jan
284 2023;54(1):E6. doi:10.3171/2022.10.Focus22606
- 285 6. Hoshide R, Feldman E, Taylor W. Cadaveric Analysis of the Kambin's Triangle. *Cureus*.
286 Feb 2 2016;8(2):e475. doi:10.7759/cureus.475
- 287 7. Hardenbrook M, Lombardo S, Wilson MC, Telfeian AE. The anatomic rationale for
288 transforaminal endoscopic interbody fusion: a cadaveric analysis. *Neurosurg Focus*. Feb
289 2016;40(2):E12. doi:10.3171/2015.10.Focus15389
- 290 8. Sakane M. Anatomical relationship between Kambin's triangle and exiting nerve root.
291 *Mini-invasive Surgery*. 2017;1:99-102. doi:10.20517/2574-1225.2017.19
- 292 9. Kouam R, Tabarestani T, Sykes D, et al. How dimensions can guide surgical planning
293 and training: a systematic review of Kambin's triangle. *Neurosurgical Focus*. 2022 In
294 Press;(January 2023 Minimally invasive surgery of lumbar spine)

- 295 10. Tabarestani TQ, Sykes DAW, Maquoit G, et al. Novel Merging of CT and MRI to Allow
296 for Safe Navigation into Kambin's Triangle for Percutaneous Lumbar Interbody Fusion—Initial
297 Case Series Investigating Safety and Efficacy. *Operative Neurosurgery*.
298 2023;10.1227/ons.0000000000000531. doi:10.1227/ons.0000000000000531
- 299 11. Wang TY, Hamouda F, Mehta VA, et al. Effect of Instrument Navigation on C-arm
300 Radiation and Time during Spinal Procedures: A Clinical Evaluation. *Int J Spine Surg*. Jun
301 2020;14(3):375-381. doi:10.14444/7049
- 302 12. Hamouda F, Wang TY, Gabr M, et al. A Prospective Comparison of the Effects of
303 Instrument Tracking on Time and Radiation During Minimally Invasive Lumbar Interbody
304 Fusion. *World Neurosurg*. Aug 2021;152:e101-e111. doi:10.1016/j.wneu.2021.05.058
- 305 13. Li Y, Wang MY. Safe Electromyography Stimulation Thresholds Within Kambin's
306 Triangle During Endoscopic Transforaminal Lumbar Interbody Fusion. *Neurosurgery*. Jul 1
307 2022;91(1):150-158. doi:10.1227/neu.0000000000001959
- 308 14. Wehab Z, Tabarestani TQ, Abd-El-Barr MM, Husain AM. Intraoperative
309 Electromyography in Awake Minimally Invasive Transforaminal Lumbar Interbody Fusion: A
310 Case Study on Nerve Activation Under the Effects of Local Anesthesia. *J Clin Neurophysiol*.
311 Nov 1 2022;39(7):e26-e29. doi:10.1097/wnp.0000000000000962
- 312 15. Morgenstern C, Yue JJ, Morgenstern R. Full Percutaneous Transforaminal Lumbar
313 Interbody Fusion Using the Facet-sparing, Trans-Kambin Approach. *Clin Spine Surg*. Feb
314 2020;33(1):40-45. doi:10.1097/bsd.0000000000000827
- 315 16. Lewandrowski K-U, Dowling Á, Calderaro AL, et al. Dysethesia due to irritation of the
316 dorsal root ganglion following lumbar transforaminal endoscopy: Analysis of frequency and

- 317 contributing factors. *Clinical Neurology and Neurosurgery*. 2020/10/01/ 2020;197:106073.
318 doi:<https://doi.org/10.1016/j.clineuro.2020.106073>
- 319 17. Pairaiturkar PP, Sudame OS, Pophale CS. Evaluation of Dimensions of Kambin's
320 Triangle to Calculate Maximum Permissible Cannula Diameter for Percutaneous Endoscopic
321 Lumbar Discectomy : A 3-Dimensional Magnetic Resonance Imaging Based Study. *J Korean*
322 *Neurosurg Soc*. Jul 2019;62(4):414-421. doi:10.3340/jkns.2018.0091
- 323 18. Choi I, Ahn JO, So WS, Lee SJ, Choi IJ, Kim H. Exiting root injury in transforaminal
324 endoscopic discectomy: preoperative image considerations for safety. *Eur Spine J*. Nov
325 2013;22(11):2481-7. doi:10.1007/s00586-013-2849-7
- 326 19. Fan G, Liu H, Wu Z, et al. Deep Learning–Based Automatic Segmentation of
327 Lumbosacral Nerves on CT for Spinal Intervention: A Translational Study. *American Journal of*
328 *Neuroradiology*. 2019;40(6):1074-1081. doi:10.3174/ajnr.A6070
- 329 20. Fan G, Liu H, Wang D, et al. Deep learning-based lumbosacral reconstruction for
330 difficulty prediction of percutaneous endoscopic transforaminal discectomy at L5/S1 level: A
331 retrospective cohort study. *International Journal of Surgery*. 2020/10/01/ 2020;82:162-169.
332 doi:<https://doi.org/10.1016/j.ijisu.2020.08.036>
- 333 21. Su Z, Liu Z, Wang M, et al. Three-dimensional reconstruction of Kambin's triangle based
334 on automated magnetic resonance image segmentation. *Journal of Orthopaedic Research*.
335 n/a(n/a)doi:<https://doi.org/10.1002/jor.25303>
- 336 22. Hurday Y, Xu B, Guo L, et al. Radiographic measurement for transforaminal
337 percutaneous endoscopic approach (PELD). *European Spine Journal*. 2017/03/01
338 2017;26(3):635-645. doi:10.1007/s00586-016-4454-z

- 339 23. Fujita M, Kawano H, Kitagawa T, et al. Preoperative Design for the Posterolateral
340 Approach in Full-Endoscopic Spine Surgery for the Treatment of L5/S1 Lumbar Disc
341 Herniation. *Neurospine*. Mar 2019;16(1):105-112. doi:10.14245/ns.1836316.158
- 342 24. Hirayama J, Hashimoto M, Sakamoto T. Clinical Outcomes Based on Preoperative
343 Kambin's Triangular Working Zone Measurements on 3D CT/MR Fusion Imaging to Determine
344 Optimal Approaches to Transforaminal Endoscopic Lumbar Discectomy. *J Neurol Surg A Cent
345 Eur Neurosurg*. Jul 2020;81(4):302-309. doi:10.1055/s-0039-3400752
- 346 25. Tenny S, Gillis CC. Spondylolisthesis. *StatPearls*. StatPearls Publishing
347 Copyright © 2023, StatPearls Publishing LLC.; 2023.
- 348 26. Kalichman L, Kim DH, Li L, Guermazi A, Berkin V, Hunter DJ. Spondylolysis and
349 spondylolisthesis: prevalence and association with low back pain in the adult community-based
350 population. *Spine (Phila Pa 1976)*. Jan 15 2009;34(2):199-205.
351 doi:10.1097/BRS.0b013e31818edcfd
- 352 27. Waguia R, Gupta N, Gamel KL, Ukachukwu A. Current and Future Applications of the
353 Kambin's Triangle in Lumbar Spine Surgery. *Cureus*. Jun 2022;14(6):e25686.
354 doi:10.7759/cureus.25686
- 355 28. Haijiao W, Koti M, Smith FW, Wardlaw D. Diagnosis of lumbosacral nerve root
356 anomalies by magnetic resonance imaging. *J Spinal Disord*. Apr 2001;14(2):143-9.
357 doi:10.1097/00002517-200104000-00009
- 358 29. Scuderi GJ, Vaccaro AR, Brusovanik GV, Kwon BK, Berta SC. Conjoined lumbar nerve
359 roots: a frequently underappreciated congenital abnormality. *J Spinal Disord Tech*. Apr
360 2004;17(2):86-93. doi:10.1097/00024720-200404000-00002

361 30. Modi HN, Shrestha U. Comparison of Clinical Outcome and Radiologic Parameters in
362 Open TLIF Versus MIS-TLIF in Single- or Double-Level Lumbar Surgeries. *Int J Spine Surg.*
363 Oct 2021;15(5):962-970. doi:10.14444/8126

364

365 **Figure Legends**

366 **Figure 1.** 3D isotropic T2-weighted MRI. Sagittal (left) and axial (right) sequences were
367 acquired at 1-mm slice thickness revealing a disc herniation at the L4-L5 level.

368 **Figure 2.** Kambin's Triangle (purple) was outlined using *Smartbrush* without the aid of the ENR
369 acting as a boundary. We used the approximation of the largest triangle that contained every part
370 of the outlined space (yellow outline) and calculated the area using the formula: $0.5 \times \text{base} \times$
371 height.

372 **Figure 3.** Individual ENRs (pink) were identified first in the axial (upper) and then sagittal
373 (lower) plane with *Smartbrush* completing segmentation based on a region-growing algorithm.
374 Each ENR was segmented bilaterally starting from where it exited the spinal cord to as far lateral
375 as possible.

376 **Figure 4.** After the nerves were visualized, the *Align* feature was again used to orient the images
377 in the direction that maximized the cross-sectional area of Kambin's triangle.

378 **Figure 5.** Kambin's triangle (orange) was segmented using its known anatomical boundaries.
379 Since the ENR (blue) had already been segmented, it helped ensure that we were not overlapping
380 Kambin's triangle with any part of the nerve. As before, we used an approximation of the largest
381 triangle that contained every part of the outlined space (yellow outline) and calculated area using
382 the formula: $0.5 \times \text{base} \times \text{height}$.

383 **Figure 6.** 3D-generated representation of all the nerves and triangles to visualize spatial
384 proximity for each lumbar level.

385 **Figure 7.** Intraoperative fluoroscopy images confirming accurate placement of instrumentation.

386 A, Pedicle screws were placed bilaterally at the proper levels using instrument-tracking. B, A
387 stimulating dilator (Spineology, St. Paul, MN) was then used to pierce through fascia and into
388 the annulus of the desired disc using the preplanned trajectory and BrainLab navigation. C, An 8
389 mm portal was placed along the same trajectory through Kambin's Triangle. D, The verify
390 balloon with omnipaque was done to ensure adequate discectomy. E, The cage was placed into
391 the disc space and expanded to 13 mm. F, Bilateral rods were used to connect the screws.

392 **Figure 8.** MRI and CT elastic fusion done intraoperatively. A, the *Spy Glass* method was done to
393 help with the alignment of the vertebrae within the range of interest (dotted white box). B, The
394 *Blending* feature was used for further confirmation of an accurate image fusion.

395 **Figure 9.** Intraoperative CT with pre-operatively segmenting objects. The ENR (orange outline)
396 and Kambin's Triangle (green outline) at the operative level were transferred over to the CT scan
397 once image fusion was completed. This allowed for trajectory planning, illustrated by the screw
398 in the top left panel.

399 **Figure 10.** Scatter line plots for both measurement techniques depicting an increase in Kambin's
400 triangle area going down the lumbar spine, but with smaller areas when using ENR
401 segmentation.

402 **Figure 11.** Segmentation images for the patient with a right conjoined L5-S1 nerve root. The
403 unconjoined side (left) revealed a triangle (highlighted purple) with an area of 121 mm², as it
404 was not inhibited by the lower S1 nerve root (orange). The conjoined side (right) revealed a

405 triangle (highlighted pink) with an area of 74.6 mm^2 , as it was inhibited by both the lower S1
406 nerve root (green) and the superior L5 nerve (blue).

407

Journal Pre-proof

Table 1. Areas of Kambin's Triangle with Nerve Segmentation

| Levels: | Average Area (mm²) | SD | Median | IQR |
|----------------|--------------------------------------|-----------|---------------|------------|
| L1-L2 | 50.0 | 12.3 | 51.6 | 15.3 |
| L2-L3 | 73.8 | 12.5 | 74.0 | 13.4 |
| L3-L4 | 83.8 | 12.2 | 87.3 | 13.9 |
| L4-L5 | 88.5 | 19.0 | 88.7 | 27.3 |
| L5-S1 | 116 | 29.3 | 112 | 44.0 |

Table 2. Demographic and Pathologic Data

| Patient # | Age | BMI | Sex | # of Pathological Levels | Type of Pathology Present |
|-------------|------|-------|-----|--------------------------|--|
| 1 | 76 | 31.6 | F | 2 | Grade 1 Spondy and Foraminal Stenosis |
| 2 | 68 | 21.6 | F | 1 | Grade 1 Spondy and Foraminal Stenosis |
| 3 | 61 | 29.7 | M | 1 | Grade 1 Spondy and Foraminal Stenosis |
| 4 | 67 | 23.6 | F | 1 | Grade 1 Spondy |
| 5 | 85 | 27.8 | M | 1 | Grade 1 Spondy and Foraminal Stenosis |
| 6 | 55 | 36.2 | F | 1 | Grade 2 Spondy |
| 7 | 65 | 31.8 | M | 1 | Grade 1 Spondy and Canal Stenosis |
| 8 | 73 | 33.8 | M | 1 | Grade 1 Spondy |
| 9 | 53 | 20.1 | M | 1 | Grade 1 Spondy and Foraminal Stenosis |
| 10 | 69 | 25.4 | M | 1 | Grade 1 Spondy and Canal Stenosis |
| 11 | 77 | 31.6 | F | 2 | Grade 1 Spondy and Facet Cysts |
| 12 | 52 | 28.5 | M | 2 | Disc Protrusion and Conjoined Nerve Root |
| 13 | 65 | 26.86 | F | 2 | Grade 2 Spondy |
| 14 | 66 | 38.74 | F | 1 | Grade 1 Spondy and Foraminal Stenosis |
| 15 | 80 | 31.87 | M | 2 | Grade 1 Spondy and Foraminal Stenosis |
| Mean | 67.2 | 28.2 | - | - | - |
| SD | 9.58 | 5.38 | - | - | - |

Table 3. Comparing the areas of Kambin's Triangle at pathologic vs. non-pathologic levels

| Levels | Mean Pathological Area (mm²) | Mean Non-Pathological Area (mm²) | P values |
|---------------|--|--|-----------------|
| L3-L4 | 82.4 ± 10.7 | 84.2 ± 12.7 | 0.75 |
| L4-L5 | 85.0 ± 17.4 | 102 ± 20.2 | 0.046* |
| L5-S1 | 99.7 ± 34.6 | 122 ± 24.7 | 0.049* |

*Significance was determined if p-value < 0.05

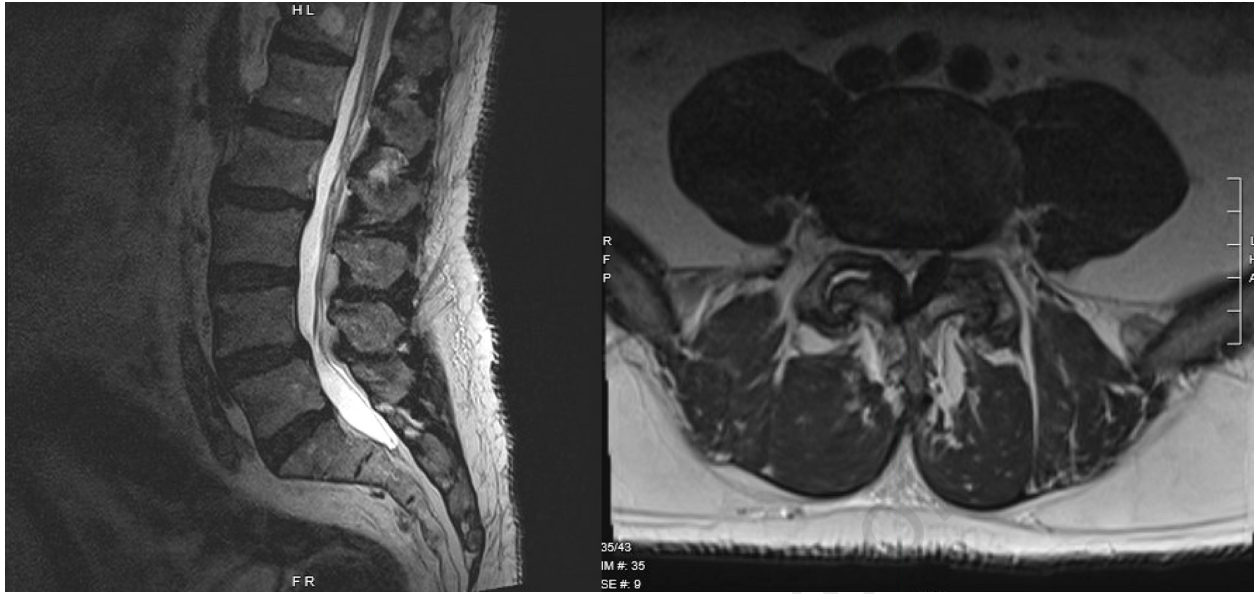
Table 4. Comparing the smaller and larger Kambin's Triangle at pathologic levels

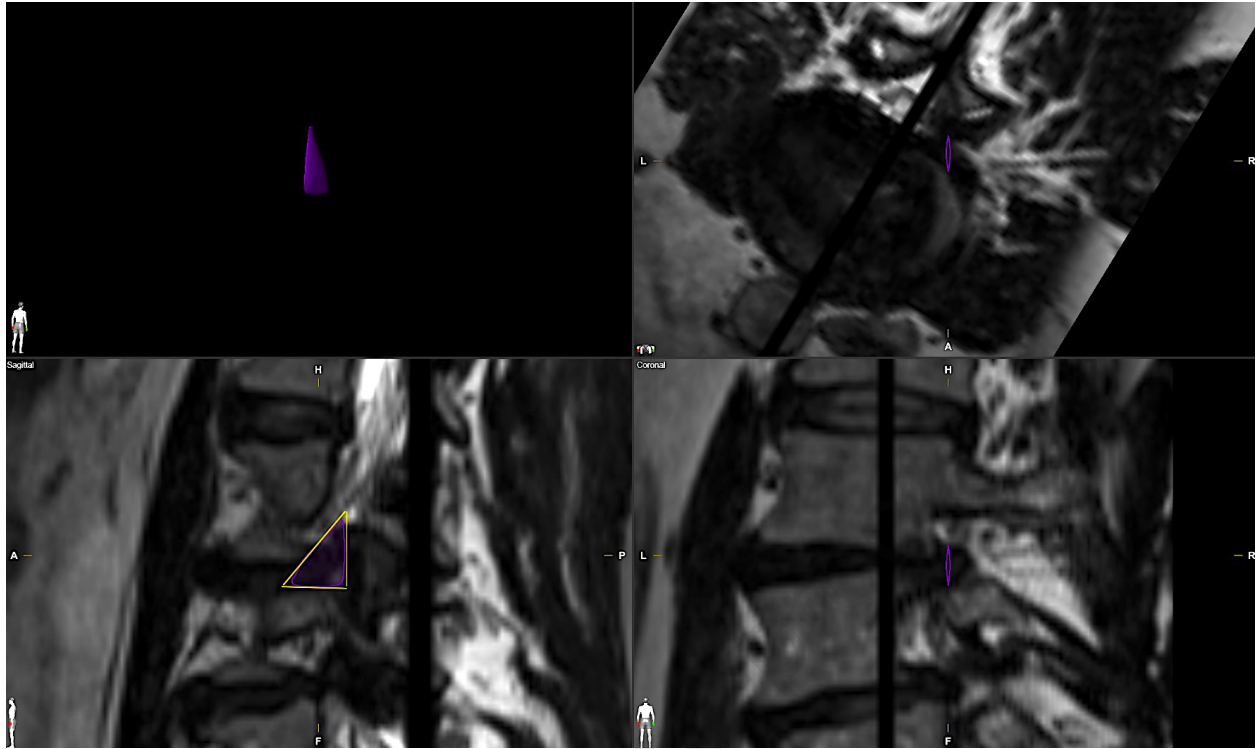
| Levels | Laterality | Mean Pathologic Area (mm²) | P Values |
|---------------|-------------------|--|-----------------|
| L3-L4 | Small Side | 79.6 ± 8.7 | 0.58 |
| | Large Side | 85.2 ± 13.7 | |
| L4-L5 | Small Side | 76.2 ± 14.5 | 0.0091* |
| | Large Side | 93.9 ± 15.9 | |
| L5-S1 | Small Side | 85.1 ± 30.8 | 0.26 |
| | Large Side | 114 ± 35.8 | |

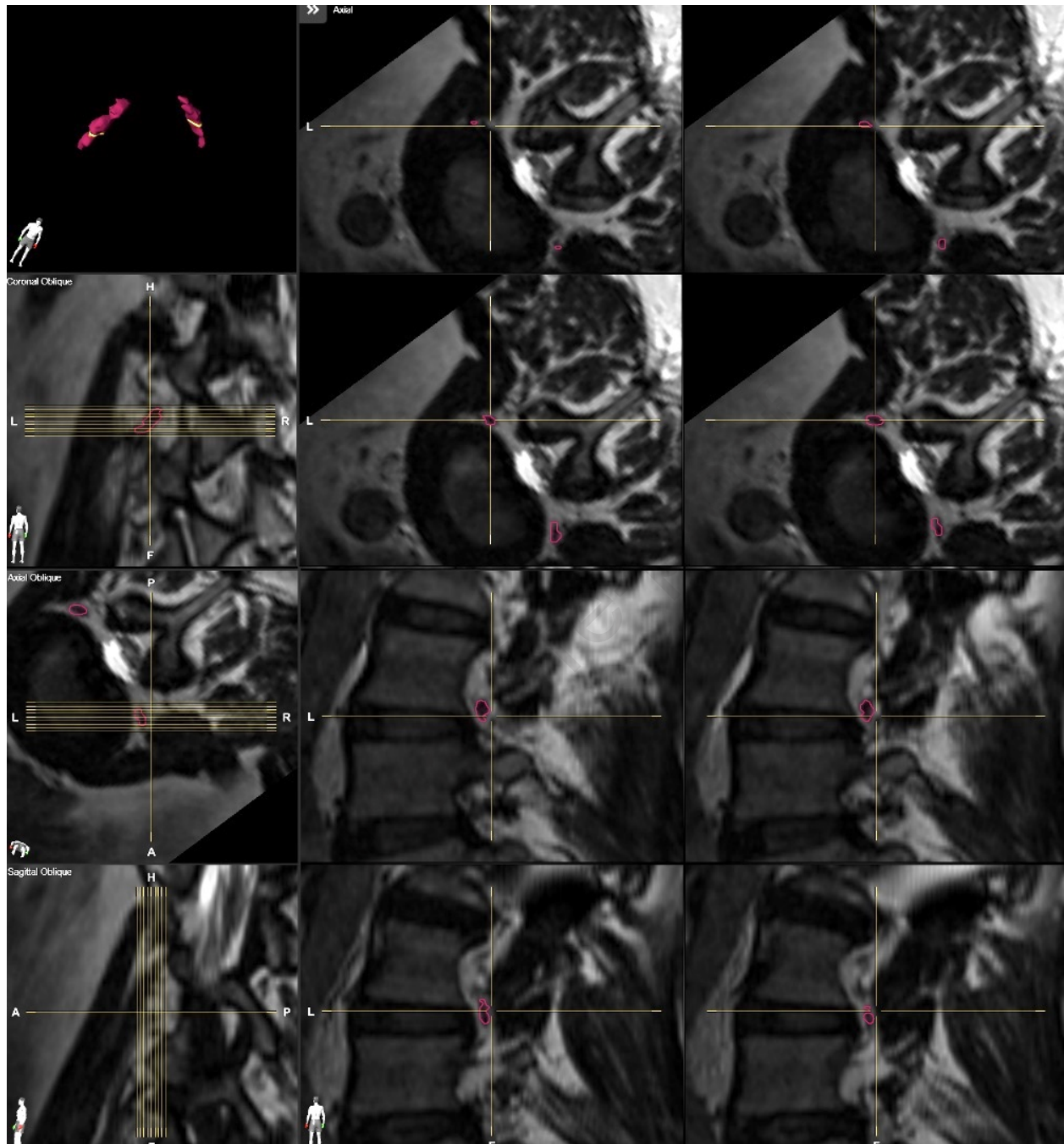
*Significance was determined if p-value < 0.05

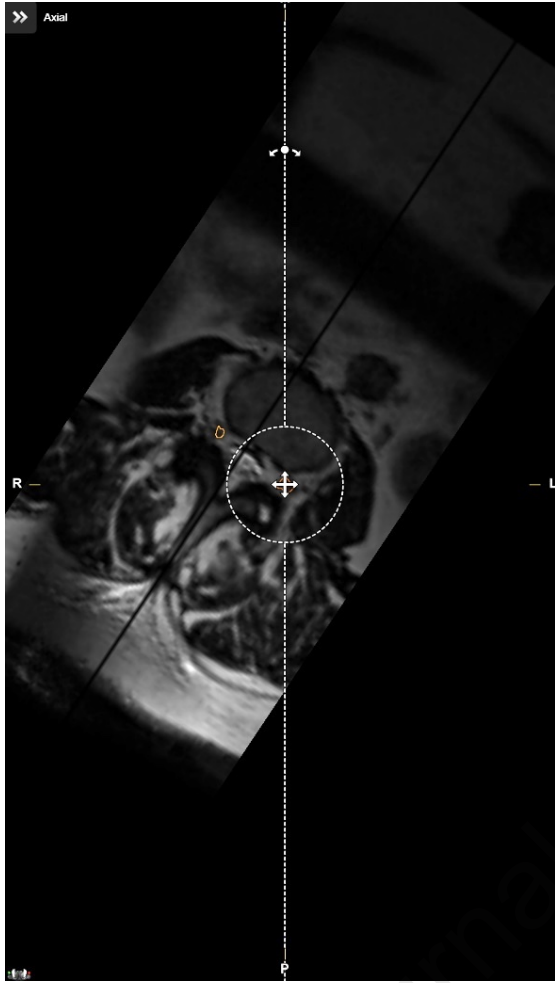
Table 5. Peri and Postoperative Data

| Patient # | Anesthesia Type | LOS (hours) | Blood Loss (ml) | Operative Time (mins) | Months to Follow-Up |
|-------------|-----------------|-------------|-----------------|-----------------------|---------------------|
| 1 | Awake | 12 | 50 | 180 | 16.5 |
| 2 | General | 24 | 10 | 183 | 1.9 |
| 3 | Awake | 14 | 25 | 160 | 13.3 |
| 4 | Awake | 14 | 50 | 140 | 12.5 |
| 5 | Awake | 34 | 25 | 184 | 14.6 |
| 6 | General | 33 | 50 | 182 | 8.2 |
| 7 | Awake | 27 | 50 | 193 | 9.9 |
| 8 | General | 48 | 150 | 210 | 6.7 |
| 9 | General | 35 | 25 | 150 | 5.8 |
| 10 | Awake | 36 | 50 | 147 | 7.3 |
| 11 | NA | NA | NA | NA | NA |
| 12 | NA | NA | NA | NA | NA |
| 13 | General | 33 | 150 | 193 | 1.5 |
| 14 | NA | NA | NA | NA | NA |
| 15 | NA | NA | NA | NA | NA |
| Mean | - | 28.2 | 57.7 | 174 | 8.9 |
| SD | - | 11.2 | 47.8 | 22.2 | 4.9 |

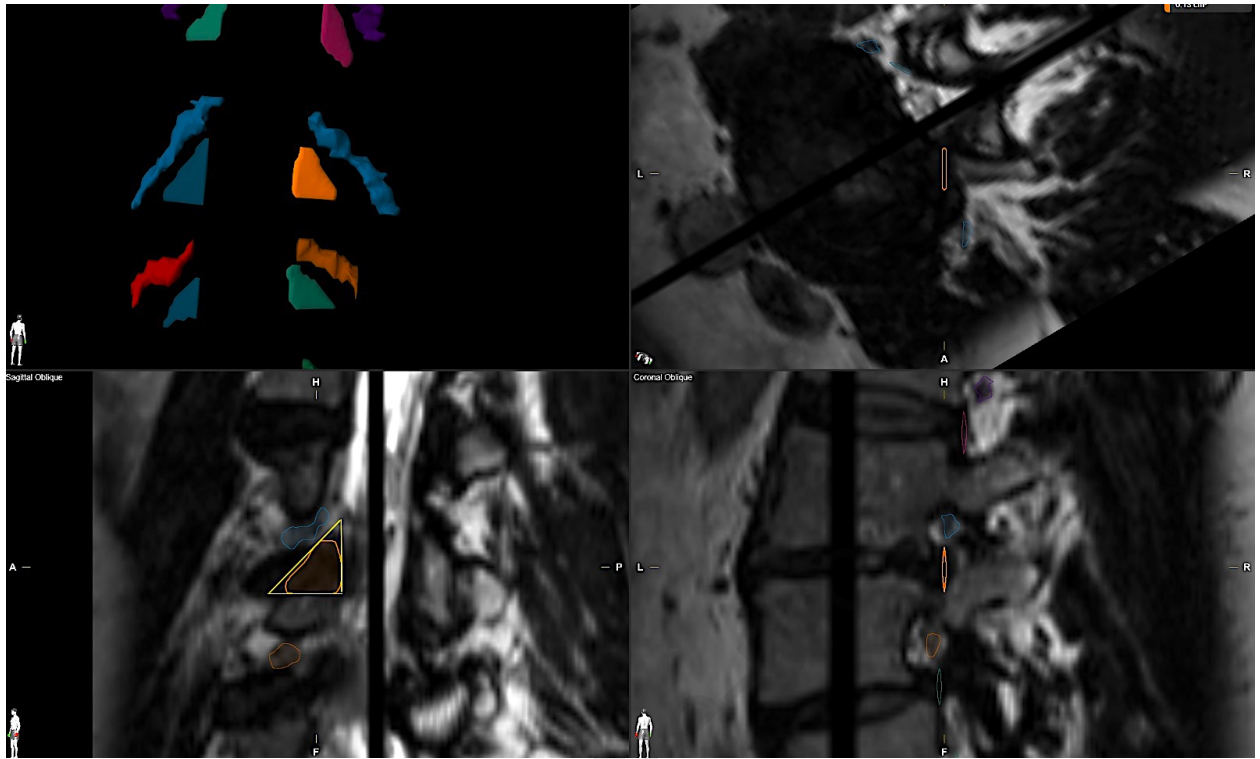








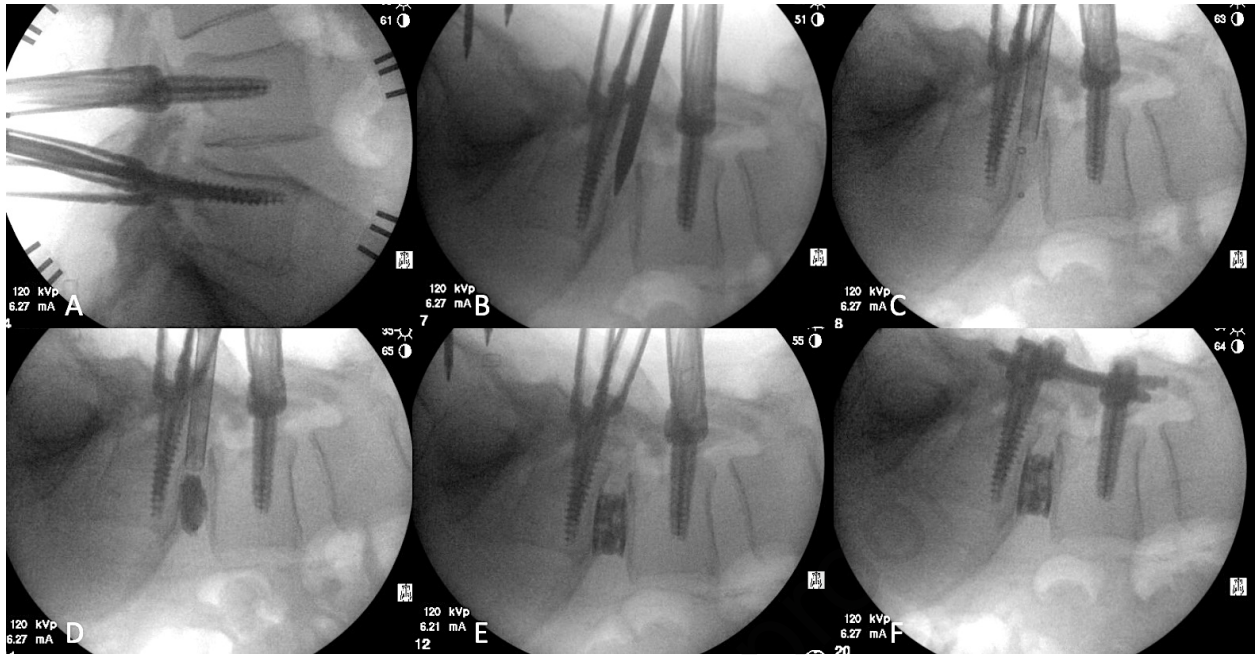
Journal Pre-proof

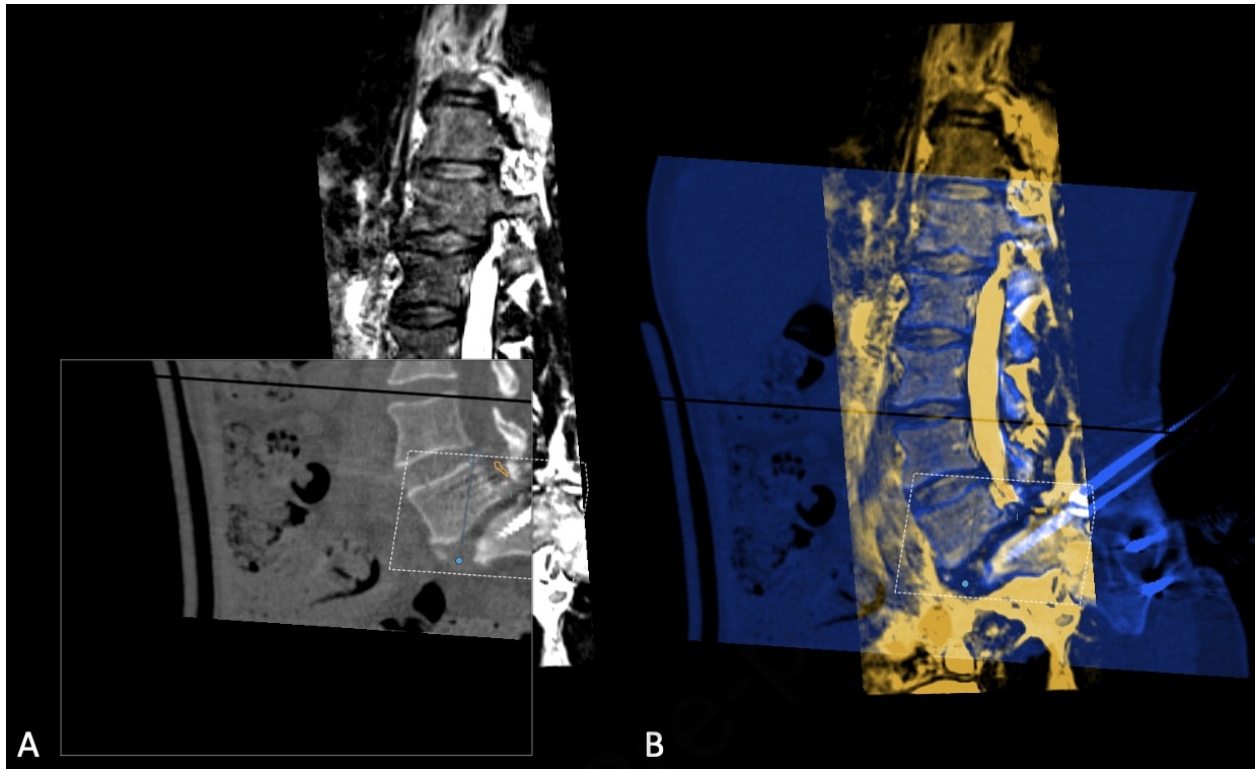


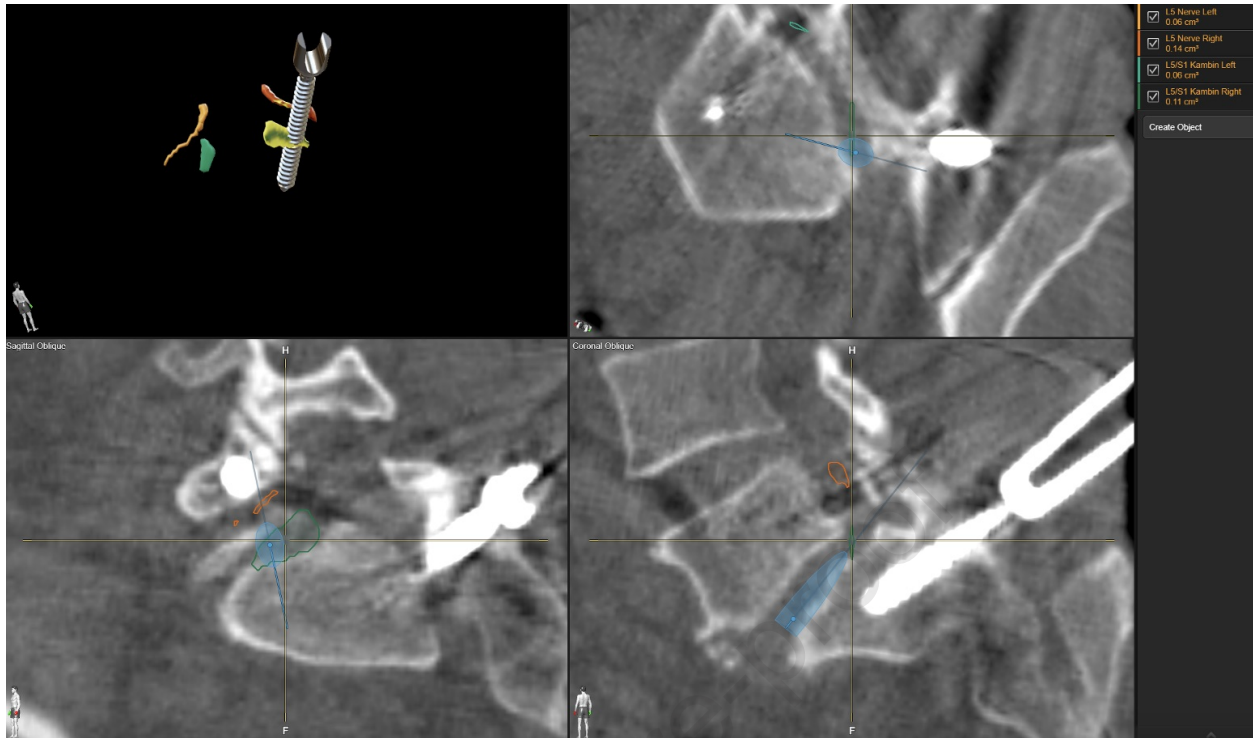
Journal Pre-proof



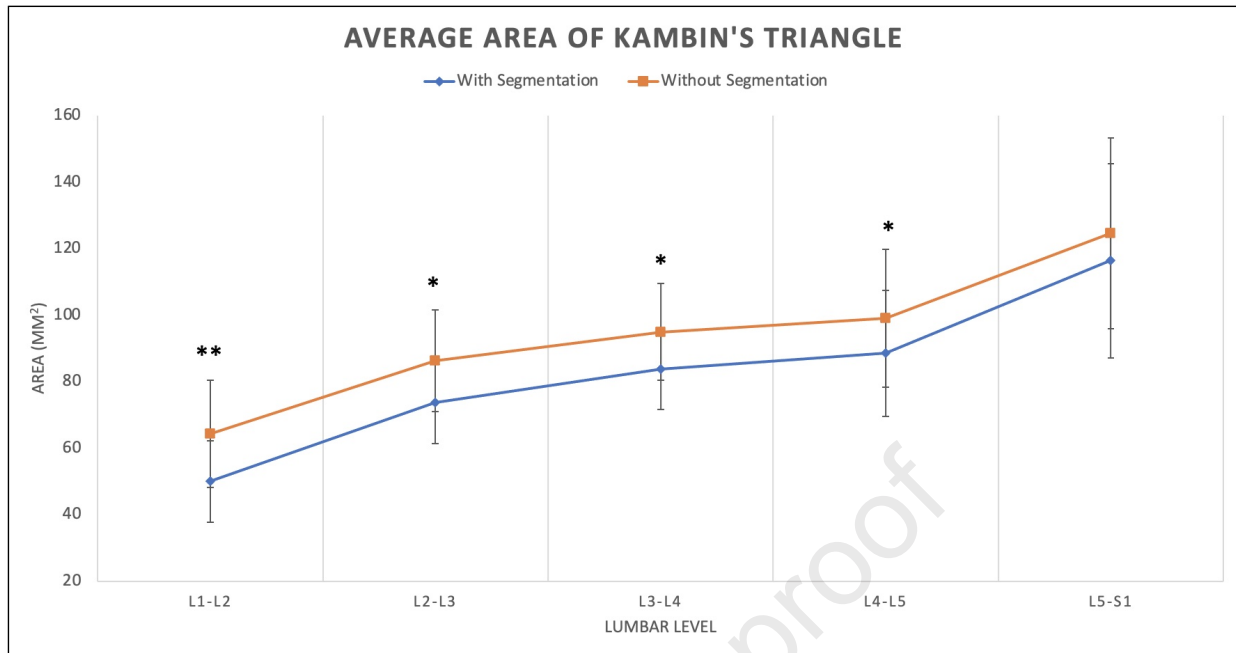
Journal Pre-proof

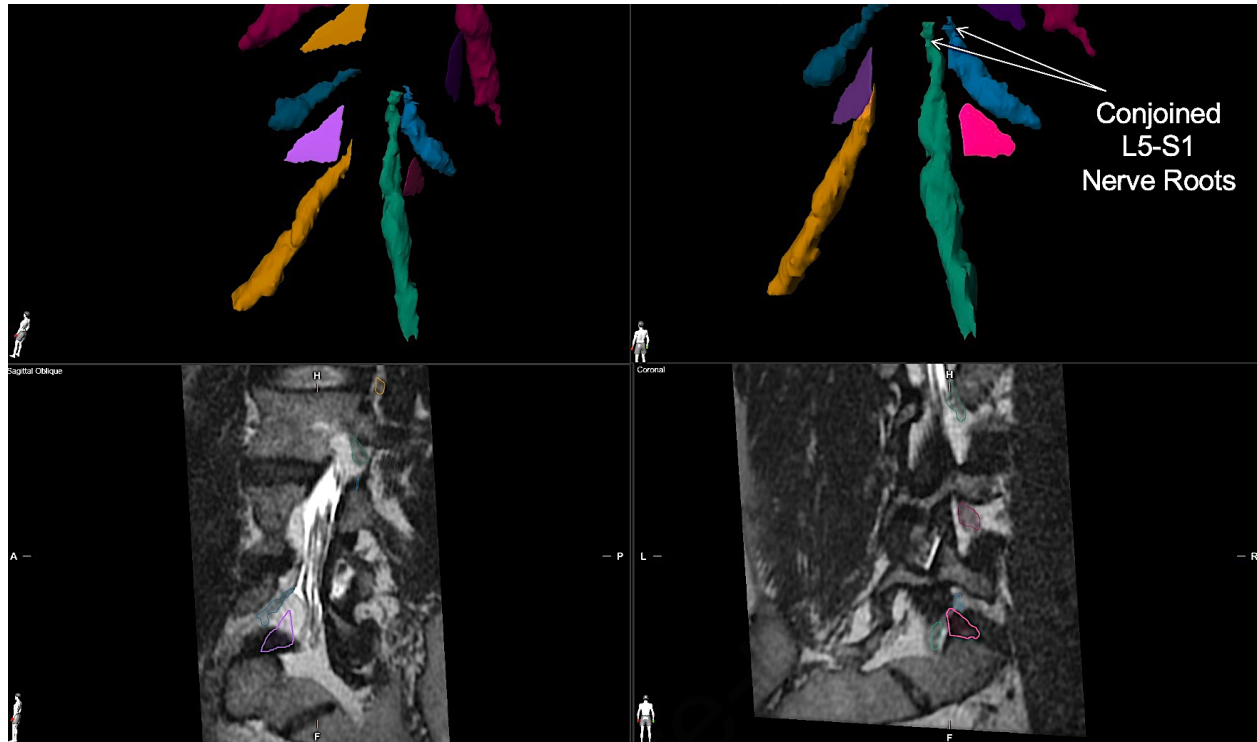






Journal Pre-proof





Abbreviations: percutaneous lumbar interbody fusion (percLIF), minimally invasive surgeries (MIS), exiting nerve root (ENR), computed tomography (CT), three-dimensional (3D), magnetic resonance imaging (MRI), electromyography (EMG), dorsal root ganglion (DRG), anterior disc height (ADH), posterior disc height (PDH)

Journal Pre-proof

Disclosures

Muhammad M. Abd-El-Barr is a consultant for Depuy Synthes, TrackX, and Spineology.

Journal Pre-proof

Author Statement

Troy Q. Tabarestani: Conceptualization; Data curation; Formal analysis; Roles/Writing - original draft; Writing - review & editing. **David A.W. Sykes:** Conceptualization; Data curation; Formal analysis; Roles/Writing - original draft; Writing - review & editing. **Romarie W. Kouam:** Conceptualization; Data curation; Formal analysis; Roles/Writing - original draft; Writing - review & editing. **David S. Salven:** Supervision; Validation; Visualization; Roles/Writing - original draft; Writing - review & editing. **Timothy Y. Wang:** Supervision; Validation; Visualization; Roles/Writing - original draft; Writing - review & editing. **Vikram A. Mehta:** Supervision; Validation; Visualization; Roles/Writing - original draft; Writing - review & editing. **Christopher I. Shaffrey:** Supervision; Validation; Visualization; Roles/Writing - original draft; Writing - review & editing. **Walter F. Wiggins:** Conceptualization; Data curation; Project administration; Resources; Supervision; Validation; Visualization; Roles/Writing - original draft; Writing - review & editing. **John H. Chi:** Conceptualization; Data curation; Project administration; Resources; Supervision; Validation; Visualization; Roles/Writing - original draft; Writing - review & editing. **Muhammad M. Abd-El-Barr:** Conceptualization; Data curation; Project administration; Resources; Supervision; Validation; Visualization; Roles/Writing - original draft; Writing - review & editing.